Article

Supramolecular Helices via Self-Assembly of 8-Oxoguanosines

Tatiana Giorgi, Stefano Lena, Paolo Mariani, Mauro A. Cremonini, Stefano Masiero, Silvia Pieraccini, Jrgen P. Rabe, Paolo Samor, Gian Piero Spada, and Giovanni Gottarelli

J. Am. Chem. Soc., **2003**, 125 (48), 14741-14749• DOI: 10.1021/ja0364827 • Publication Date (Web): 07 November 2003

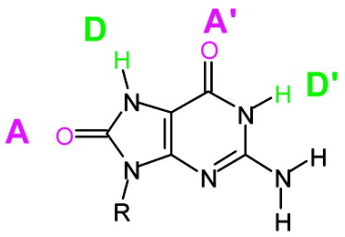

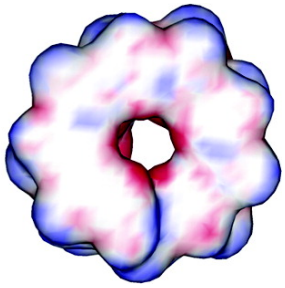

More About This Article

Additional resources and features associated with this article are available within the HTML version:

- Supporting Information
- Links to the 14 articles that cite this article, as of the time of this article download
- Access to high resolution figures
- Links to articles and content related to this article
- Copyright permission to reproduce figures and/or text from this article

View the Full Text HTML

J|A|C|S
ARTICLES
Published on Web 11/07/2003

Supramolecular Helices via Self-Assembly of 8-Oxoguanosines

Tatiana Giorgi,[†] Stefano Lena,[†] Paolo Mariani,[‡] Mauro A. Cremonini,[§] Stefano Masiero,[†] Silvia Pieraccini,[†] Jürgen P. Rabe,[||] Paolo Samorì,*[,||,#] Gian Piero Spada,*[,†] and Giovanni Gottarelli*[,†]

Alma Mater Studiorum−Università di Bologna, Dipartimento di Chimica Organica "A. Mangini", via San Donato 15, 40127 Bologna, Italy, Università Politecnica delle Marche, Istituto di Scienze Fisiche and INFM Istituto Nazionale per la Fisica della Materia, via Ranieri 65, 60131 Ancona, Italy, Alma Mater Studiorum−Università di Bologna, Dipartimento di Scienze degli Alimenti, via Ravennate 1020, 47023 Cesena, Italy, Department of Physics, Humboldt University Berlin, Newtonstrasse 15, D-12489 Berlin, Germany, and Istituto per la Sintesi Organica e la Fotoreattività, Consiglio Nazionale delle Ricerche, via Gobetti 101, 40129 Bologna, Italy

Received June 3, 2003; E-mail: giovanni.gottarelli@unibo.it; gianpiero.spada@unibo.it; samori@isof.cnr.it

Abstract: The cooperative effect of solvophobic interactions and hydrogen bonding has been exploited to self-assemble supramolecular helical architectures of 8-oxoguanosines in different environments. This self-assembly into helical structures is completely different from that of the parent guanosines which, in the same experimental conditions, form flat, ribbonlike structures. While optical microscopy and X-ray diffraction suggest a chiral columnar aggregate in the LC phase, NMR and Circular Dichroism reveal the presence of a helical structures in solution. Scanning Tunneling Microscopy made it possible to visualize hexagonally arranged G-quartets on graphite, which are sections of the helices packed with their long axis perpendicular to the basal plane of the substrate. Due to their rectifying electrical properties, such helices are interesting for fabricating (opto)electronic biodevices.

Introduction

Harmonizing the functionalities of individual moieties in a supramolecular network represents a versatile approach for developing well-defined polymeric architectures with pre-programmed conformations and tailored properties.[1] In this frame, one major goal is to use cooperatively weak interactions for generating self-organized helical assemblies.[2,3] This approach allows for the construction of synthetic supramolecular helices, simultaneously exploiting solvophobic interactions and hydrogen bonding, thereby replicating the interactions that contribute to the formation of the double-stranded helical structure of DNA.[3] Lipophilic guanosine derivatives

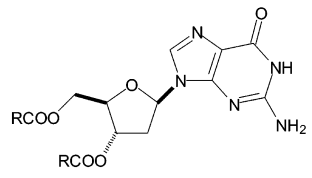

R = C_9H_{19} **1**
R = *p*-($C_{12}H_{25}O$)Ph **2**
R = C_2H_5 **3**

(e.g., **1**−**3**) are capable of self-assembling into different structures depending on the experimental conditions. In the presence of certain ions, they can form G-quartet-based octamers or columnar aggregates (supramolecular polymers) depending on the concentration of the ion and nucleobase. The ions act as templates and they are located between the quartets (Figure 1). In these assembled structures, both syn and anti orientations of the base around the glycosidic bond have been observed.[4,5]

[†] Alma Mater Studiorum−Università di Bologna, Dipartimento di Chimica Organica "A. Mangini".
[‡] Università Politecnica delle Marche.
[§] Alma Mater Studiorum − Università di Bologna, Dipartimento di Scienze degli Alimenti.
[||] Humboldt University Berlin.
[#] Istituto per la Sintesi Organica e la Fotoreattività.

(1) Lehn, J.-M. *Science* **2002**, *295*, 2400. Balzani, V.; Credi, A.; Raymo, F. M.; Stoddart, J. F. *Angew. Chem.* **2000**, *111*, 3484; *Angew. Chem., Int. Ed.* **2000**, *39*, 3348. Stupp, S. I.; LeBonheur, V.; Walker, K.; Li, L. S.; Huggins, K. E.; Keser, M.; Amstutz, A. *Science* **1997**, *276*, 384.
(2) Rowan, A. E.; Nolte, R. J. M. *Angew. Chem., Int. Ed.* **1998**, *37*, 63. Nelson, J. C.; Saven, J. G.; Moore, J. S.; Wolynes, P. G. *Science* **1997**, *277*, 1793. Berl, V.; Huc, I.; Khoury, R. G.; Krische, M. J.; Lehn, J.-M. *Nature* **2000**, *407*, 720. Prins, L. J.; Timmerman, T.; Reinhoudt, D. N. *J. Am. Chem. Soc.* **2001**, *123*, 10 153. Bong, D. T.; Clark, T. D.; Granja, J. R.; Ghadiri, M. R. *Angew. Chem., Int. Ed.* **2001**, *40*, 988. Phillips, K. E. S.; Katz, T. J.; Jockusch, S.; Lovinger, A. J.; Turro, N. J. *J. Am. Chem. Soc.* **2001**, *123*, 11 899. Fenniri, H.; Mathivanan, P.; Vidale, K. L.; Sherman, D. M.; Hallenga, K.; Wood, K. V.; Stowell, J. G. *J. Am. Chem. Soc.* **2001**, *123*, 3854. Oda, R.; Huc, I.; Schutz, M.; Candau, S. J.; MacKintosh, F. C. *Nature* **1999**, *399*, 566. Orr, G. W.; Barbour, L. J.; Atwood, J. L. *Science* **1999**, *285*, 1049. Percec, V.; Glodde, M.; Bera, T. K.; Miura, Y.; Shiyanovskaya, I.; Singer, K. D.; Balagurusamy, V. S. K.; Heiney, P. A.; Schnell, I.; Rapp, A.; Spiess, H.-W.; Hudson, S. D.; Duan, H. *Nature* **2002**, *419*, 384. Bushey, M. L.; Hwang, A.; Stephens, P. W.; Nuckolls, C. *Angew. Chem., Int. Ed.* **2002**, *41*, 2828. Schenning, A. P. H. J.; Kilbinger, A. F. M.; Biscarini, F.; Cavallini, M.; Cooper, H. J.; Derrick, P. J.; Feast, W. J.; Lazzaroni, R.; Leclere, P.; McDonell, L. A.; Meijer, E. W.; Meskers, S. C. J. *J. Am. Chem. Soc.* **2002**, *124*, 1269. Engelkamp, H.; Middelbeek, S.; Nolte, R. J. M. *Science* **1999**, *284*, 785.
(3) Hirschberg, J. H. K. K.; Brunsveld, L.; Ramzi, A.; Vekemans, J. A. J. M.; Sijbesma, R. P.; Meijer, E. W. *Nature* **2000**, *407*, 167.

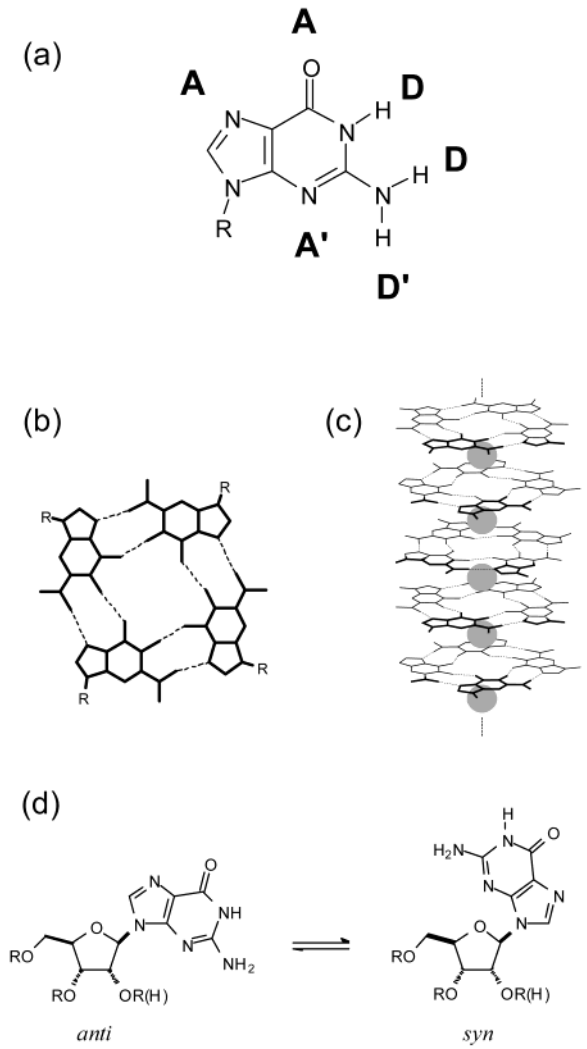

Figure 1. Donor/acceptor sites in the guanine moiety (a), the G-quartet arrangement (b) and the columnar ion-directed self-assembly (c). A simplified sketch of *syn* and anti conformations (d).

Sessler has recently shown[6] that attaching a sterically demanding group to the C(8)-position (derivative **4**), enables the molecules to self-associate into G-quartets, both in the solid state and in solution, even in the absence of the template metal cations. Only the syn stereochemistry was observed for the G-quartets formed from **4**.

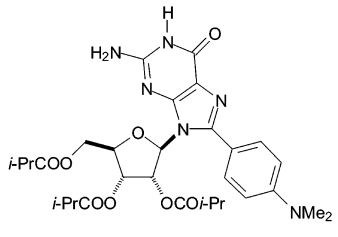

4

In the absence of metal templates, guanosines without a C(8)-substituent self-assemble, both in solution and in the solid state, into ribbonlike architectures (Figure 2) with an anti orientation of the base around the glycosidic bond.[7−9]

These ribbon structures are interesting: they are the building blocks for new lyotropic mesophases formed in organic solvents.[8,10,11] In the solid state, the ribbons, by bridging gold electrodes, are photoconductive.[12] More interestingly, these ribbons also display rectifying properties.[13] A field effect transistor, based on this supramolecular structure, has been recently described.[14] Furthermore, crystals of the ribbon obtained from derivative **3** generate second harmonics.[15] It is worth noticing that ribbon II is dipolar and that in the crystal, due to the parallel packing of the ribbons, these dipoles are parallel.[8]

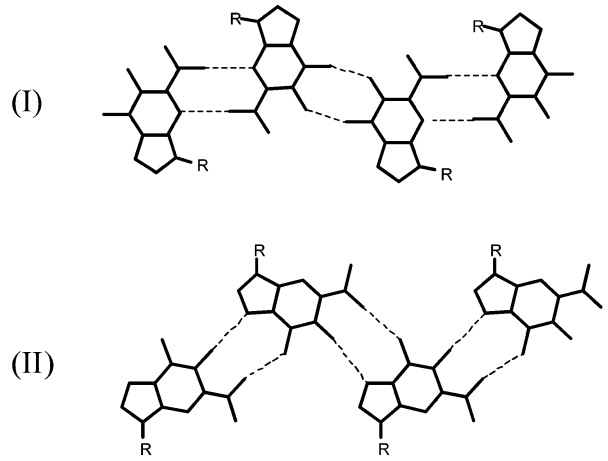

Figure 2. Structural motifs of the two ribbonlike supramolecular assemblies of guanosine derivatives in the absence of cations.[7,8]

In an effort to modify and enhance these unique electronic properties, we broadened our scope to investigate 8-substituted lipophilic G-derivatives. Here, we report the synthesis of different 8-substituted guanosines and the study of their self-assembly behavior under different environmental conditions.

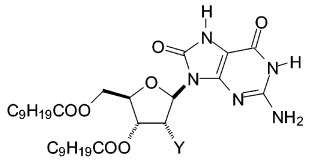

Y = H **5**
Y = $OCOC_9H_{19}$ **6**

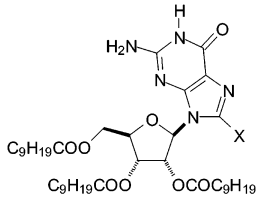

X = SCH_3 **7**
X = Br **8**

8-Oxo derivatives **5** and **6** are models for 8-oxoguanine, a species formed during DNA oxidation.[16,17] Interestingly, 8-ox-

(4) Marlow, A. L.; Mezzina, E.; Spada, G. P.; Masiero, S.; Davis, J. T.; Gottarelli, G. *J. Org. Chem.* **1999**, *64*, 5116. Forman, S. L.; Fettinger, J. C.; Pieraccini, S.; Gottarelli, G.; Davis, J. T. *J. Am. Chem. Soc.* **2000**, *122*, 4060. Mezzina, E.; Mariani, P.; Itri, R.; Masiero, S.; Pieraccini, S.; Spada, G. P.; Spinozzi, F.; Davis, J. T.; Gottarelli, G. *Chem. Eur. J.* **2001**, *7*, 388. Shi, X.; Fettinger, J. C.; Davis, J. T. *Angew. Chem., Int. Ed.* **2001**, *40*, 2827. Wong, A.; Fettinger, J. C.; Forman, S. L.; Davis, J. T.; Wu, G. J. *J. Am. Chem. Soc.* **2002**, *124*, 742.
(5) The same is true for water-soluble compounds in the solid state and in solution; see, for example: Kang, C.; Zhang, X.; Ratliff, R.; Moyzis, R.; Rich, A. *Nature* **1992**, *356*, 126. Laughlan, G.; Murchie, A. J. H.; Norman, D. G.; Moore, M. H.; Moody, P. C. E.; Lilley, D. M. J.; Luisi, B. *Science* **1994**, *265*, 520. Smith, F. W.; Feigon, J. *Nature* **1992**, *356*, 164. Smith, F. W.; Lau, F. W.; Feigon, J. *Proc. Natl. Acad. Sci. U.S.A.* **1994**, *91*, 10 546.
(6) Sessler, J. L.; Sathiosatham, M.; Doerr, K.; Lynch, V.; Abboud, K. H. *Angew. Chem., Int. Ed.* **2000**, *39*, 1300.

oguanines possess oxidation potentials (E_{ox}) that are even lower than those of guanines,[17,18] which have the lowest E_{ox} of the primary DNA nucleobases. This lowered E_{ox} for **5** and **6** should further enhance the conductive properties of guanosine based architectures.

Moreover, we have extended our studies to include the 8-methylthio substituent (**7**), in an attempt to further enhance the dipolar character of guanosine. Finally, the 8-bromo derivative **8** was used as a reference compound, the syn conformation of 8-bromoguanosine being reported in the literature.[19,20]

Of these compounds (**5**−**8**), only the 8-oxo derivatives **5** and **6** self-assemble to give lyotropic mesophases in organic solvents. This is basically correlated to the presence of a new lactamic function in the five-membered ring which generates new hydrogen bonding architectures. Although optical microscopy and X-ray diffraction allowed us to cast light on the behavior of **5** and **6** in the liquid crystalline phase, NMR and Circular Dichroism were employed to investigate the formation of supramolecular assemblies in solution. The use of Scanning Tunneling Microscopy also made it possible to gain insight into the self-assembly at surfaces.

The results indicate the formation of a continuous helical structure. This structure is interesting as it is a new architecture formed by a biologically important molecule; furthermore, the helix could explain the rectifying properties of cast films of 8-oxoguanosine derivatives.[13]

Liquid Crystalline Phases of 8-Oxo Derivatives. Among the 8-substituted derivatives **5**−**8**, only the 8-oxo compounds **5** and **6** displayed lyotropic liquid crystalline properties. The LC properties of **5** and **6** were, however, quite different from those of the 8-unsubstituted derivatives reported in ref 8. Optical microscopy reveals the presence of two birefringent phases,[21] depending on the percentage of **5** and **6** in heptane or hexane: they exist at $c = 2-12$ and $c > 12\%$ (w/w) (c being the weight of the guanosine derivative over the total weight of the sample).

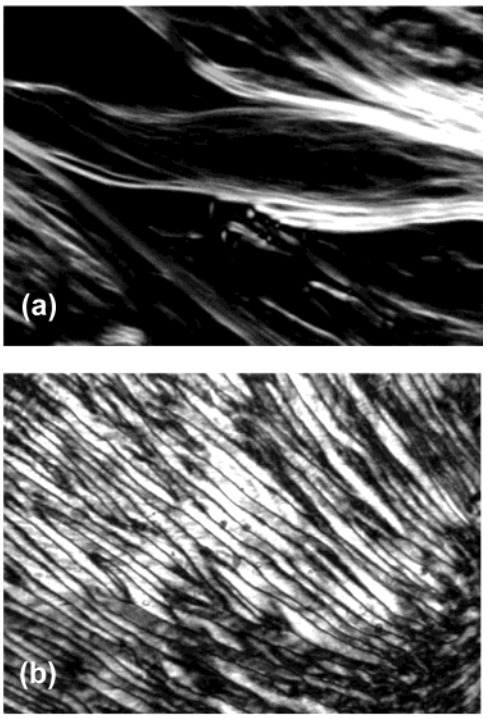

Figure 3. Optical textures of the two LC phases observed for **6** in heptane at $c = 8$ (a) and 15% (w/w) (b) (Magnification 250×).

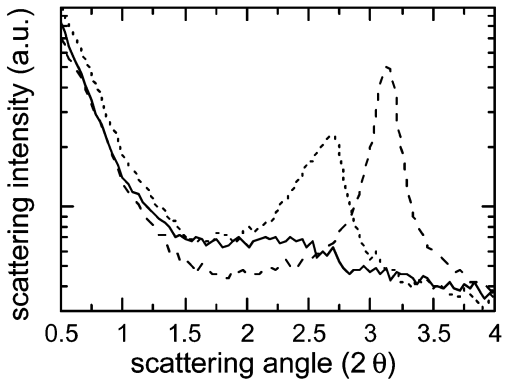

Figure 4. Low-angle X-ray diffraction profiles obtained for derivative **6** in hexane at $c = 3\%$ (full line) 10% (dotted line) and 20% (dashed line).

X-ray diffraction experiments confirm the presence of two different phases (see next paragraph). In contrast, unsubstituted G-derivatives show only a single phase with two-dimensional square symmetry, based on the previously described G-ribbons.[8]

X-ray diffraction measurements have been performed as a function of the concentration of **5** or **6** in hexane. The experimental diffraction data for the two systems are practically superimposable, thus only the results obtained from **6** will be described. Typical low angle X-ray diffraction profiles obtained at different compositions are shown in Figure 4, whereas Figure 5 shows a complete scattering profile obtained at high concentration.

The analysis has been carried out considering separately the low and the high angle diffraction regions, since from the

(7) Gottarelli, G.; Masiero, S.; Mezzina, E.; Pieraccini, S.; Rabe, J. P.; Samorì, P.; Spada, G. P. *Chem. Eur. J.* **2000**, *6*, 3242.
(8) Giorgi, T.; Grepioni, F.; Manet, I.; Mariani, P.; Masiero, S.; Mezzina, E.; Pieraccini, S.; Saturni, L.; Spada, G. P.; Gottarelli, G. *Chem. Eur. J.* **2002**, *8*, 2143.
(9) Araki, K.; Takasawa, R.; Yoshikawa, I. *Chem. Commun.* **2001**, 1826.
(10) Also, lipophilic derivatives of folic acid give ribbonlike assembled species and liquid crystalline phases: Kato, T. *Science* **2002**, *295*, 2414, and references therein.
(11) Gottarelli, G.; Masiero, S.; Mezzina, E.; Pieraccini, S.; Spada, G. P.; Mariani, P. *Liq. Cryst.* **1999**, *26*, 965.
(12) Rinaldi, R.; Branca, E.; Cingolani, R.; Masiero, S.; Spada, G. P.; Gottarelli, G. *Appl. Phys. Lett.* **2001**, *78*, 3541.
(13) Rinaldi, R.; Branca, E.; Cingolani, R.; De Felice, R.; Calzolari, A.; Molinari, E.; Masiero, S.; Spada, G. P.; Gottarelli, G.; Garbesi, A. *Ann. N. Y. Acad. Sci.* **2002**, *960*, 184. Rinaldi, R.; Maruccio, G.; Biasco, A.; Arima, V.; Cingolani, R.; Giorgi, T.; Masiero, S.; Spada, G. P.; Gottarelli, G. *Nanotechnology* **2002**, *13*, 398.
(14) Maruccio, G.; Visconti, P.; Arima, V.; D'Amico, S.; Biasco, A.; D'Amone, E.; Cingolani, R.; Rinaldi, R.; Masiero, S.; Giorgi, T.; Gottarelli, G. *Nano Lett.* **2003**, *3*, 479.
(15) Gottarelli, G.; Taliani, C.; Spada, G. P., manuscript in preparation.
(16) Kasai, H.; Yamaizumi, Z.; Berger, M.; Cadet, J. *J. Am. Chem. Soc.* **1992**, *114*, 9692. Miller, J. H.; Fan-Chiang, C.-C. P.; Straatsma, T. P.; Kennedy, M. A. *J. Am. Chem. Soc.* **2003**, *125*, 6331.
(17) Burrows, C. J.; Muller, J. G. *Chem. Rev.* **1998**, *98*, 1109. White, B.; Smyth, M. R.; Stuart, J. D.; Rusling, J. F. *J. Am. Chem. Soc.* **2003**, in press.
(18) Berger, M.; Anselmino, C.; Mouret, J.-F.; Cadet, J. J. *J. Liq. Cromatogr.* **1990**, *13*, 929. Goyal, R. N.; Jain, N.; Garg, D. K. *Bioelectrochem. Bioenerg.* **1997**, *43*, 105. Ikeda, H.; Saito, I. *J. Am. Chem. Soc.* **1999**, *121*, 10 836.
(19) Saenger, W. *Principles of Nucleic Acid Structure*; Springer-Verlag: New York, 1984; p 21. See also: Dias, E.; Battiste, J. L.; Williamson, J. R. *J. Am. Chem. Soc.* **1994**, *116*, 4479. Altona, C.; Sundaralingam, M. *J. Am. Chem. Soc.* **1972**, *94*, 8205.
(20) Polissiou, M.; Theophanides, T. *Inorg. Chim. Acta* **1987**, 195.
(21) Although the picture of the high-concentration phase shows a "herringbone" texture observed in many hexagonal phases, including those formed by guanylates (see, e.g., Spada, G. P.; Carcuro, A.; Colonna, F. P.; Garbesi, A.; Gottarelli, G. *Liq. Cryst.* **1988**, *3*, 651) and DNA (see, e. g., Livolant, F.; Levelut, A. M.; Doucet, J.; Benoit, J. P. *Nature* **1989**, *339*, 724), the micrograph of the more diluted system does not show textures typical enough to allow an unambiguous assignment.

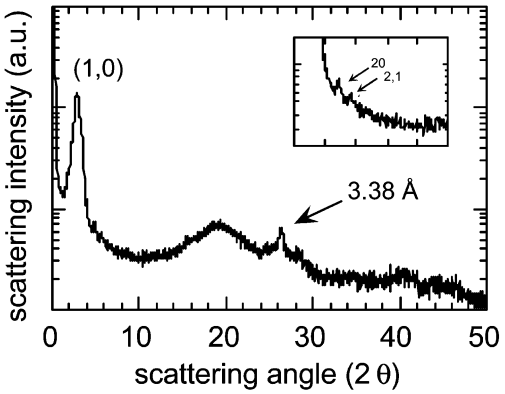

Figure 5. X-ray diffraction profile obtained from derivative **6** in hexane at $c = 20\%$. The low angle diffraction peaks have been indexed according to a 2D hexagonal packing (in the inset, the diffraction profile in the 2θ region between 2 and 12° has been expanded for clarity); the high angle peak referring to the 8-oxoguanosine stacking is indicated by the arrow. The large band centered at ca. 19.5° (around 4.6 Å) reflects the disordered nature of the hexane and of the aliphatic side chains.

former, the crystalline lattice and symmetry, as well as information on the long-range organization of the structure elements, can be derived. From the high-angle region, information on the short-range arrangement inside the structural elements can be obtained.[22,23] For concentrations of **6** ranging between 3 and 12%, a diffuse band was observed in the low angle X-ray diffraction profile. The position, width, and intensity of this broad band changes with the concentration, indicating that removal of the solvent determines both a continuous decrease of the repetition distance and an increase of the sample's long-range order. This result indicates of the presence of a poorly ordered liquid crystalline phase of a nematic or cholesteric nature. No peaks were detected in the high angle region, suggesting that order inside the structural elements is low. The low concentration of scattering particles in this condition might also explain this absence of diffraction peaks.

At concentrations of **6** higher than 12%, a series of diffraction peaks appear in the X-ray profile. According to the birefringent viscous liquid observed in the same concentration range by polarizing microscopy, the characteristic diffraction confirms the liquid-crystalline nature of the sample, as both thermotropic and lyotropic liquid crystals show an intrinsic long-range disorder.[22−25] In particular, the low-angle X-ray diffraction region is dominated by a very strong peak, whose position depends on the solvent concentration. Higher order diffraction peaks can be detected using very long exposure times (see Figure 5): at least 2 more peaks were detected, providing help in the assessment of the lattice symmetry.[22,23] The peak reciprocal spacings are, in fact, in the ratio of $1{:}\sqrt{3}{:}\sqrt{4}$, indicating a two-dimensional hexagonal packing of the structural elements. A characteristic peak, centered at about 3.4 Å, is observed in the high angle region. According to previous results,[24,25] the presence of this peak indicates the columnar,

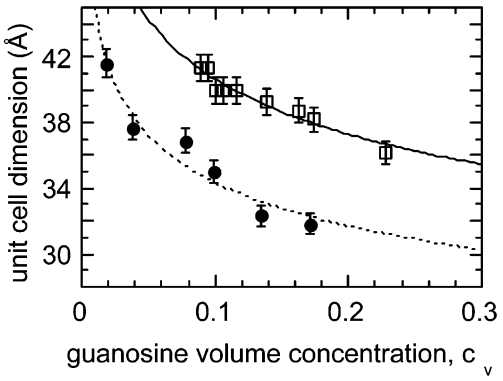

Figure 6. Dependence on concentration of the dimension of the unit cell measured in the two derivatives **5** (square) and **6** (circle) in hexane.[26]

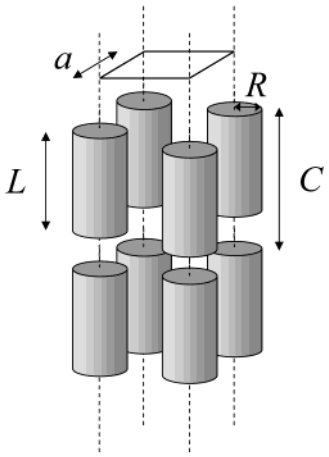

Figure 7. Representation of the hexagonal phase with the quantities defined in the text.

discotic nature of the mesophase, characterized by the regular stacking of 8-oxoguanosine, probably bonded in quartets, at the typical distance of 3.4 Å.

Therefore, the ordered liquid crystalline phase possesses a columnar hexagonal structure, with parallel elongated columnar elements (rods) consisting of stacked oxoguanosines. These rods are embedded in a hydrocarbon matrix formed by the hexane solvent and by the aliphatic side chains, which are responsible for the broad scattering band observed at about 4.4 Å (2θ about 20°). The absence of extra peaks in the low-angle X-ray diffraction profile indicates the absence of a long-range three-dimensional order. In other words, no correlation exists in the direction perpendicular to the two-dimensional cell.

According to the lattice symmetry, the dimensions of the unit cell a have been derived for **5** and **6**:[22] the observed values as a function of the concentration are reported in Figure 6. From these data, some important structural information can be derived. In the hexagonal structure (see Figure 7), the projection on the plane perpendicular to the rod axis defines the two-dimensional lattice, i.e., the unit cell a corresponds to the inter-columnar distance. Assuming the columns have a circular section with radius R (the radius of the guanosine column) and a length L, the relation between the cross-sectional area of the cylinder and the 2-dimensional hexagonal unit cell surface is as follows[22,23]

$$\pi R^2 L = C\,(\sqrt{3}/2)a^2\,c_v \qquad (1)$$

where c_v is the volume concentration of the lipophilic guanosine

(22) Luzzati, V. In *Biological Membranes*; Chapman, D., Ed.; Academic Press: London, 1968; p 71.
(23) Gottarelli, G.; Spada, G. P.; Mariani, P. In *Crystallography of Supramolecular Compounds*; Tsoucaris, G., Atwood, J. L., Lipkowski, J., Eds.; Kluwer: Netherlands, 1996; p 307.
(24) Mariani, P.; Mazabard, C.; Garbesi, A.; Spada, G. P. *J. Am. Chem. Soc.* **1989**, *111*, 6369. Bonazzi, S.; Capobianco, M.; De Morais, M. M.; Garbesi, A.; Gottarelli, G.; Mariani, P.; Ponzi Bossi, M. G.; Spada, G. P.; Tondelli, L. *J. Am. Chem. Soc.* **1991**, *113*, 5809.
(25) Pieraccini, S.; Gottarelli, G.; Mariani, P.; Masiero, S.; Saturni, L.; Spada, G. P. *Chirality* **2001**, *13*, 7.

derivative (obtained from the weight concentration, using 0.92, 0.95, and 1.45 cm^3/g as the specific volume[27] for **5**, **6** and hexane, respectively), and *C* is the average interaxial distance between rod centers (normal to the 2D cell plane). The ratio *L/C* gives essentially the fraction of solvent in the *C* direction. For rodlike elements having an infinite length, $L/C = 1$ and the concentration dependence of the unit cell is $c_v^{-1/2}$. For finite rodlike objects undergoing isotropic swelling (i.e., on dilution, the interparticle distances uniformly increase in all three dimensions) $L/C = R/a$, and thus

$$a = (2\pi R^3/\sqrt{3})^{1/3}\, c_v^{-1/3} \qquad (2)$$

Therefore, c_v exponents $-1/2$ and $-1/3$ can be considered as fingerprints of interparticle distances decreasing in a plane (2D swelling) or isotropically in the volume around the particles in all three dimensions (3D swelling), respectively. It should be noticed that if the length of the rod particles depends on the concentration, or if the interparticle distances change anisotropically with concentration, then the *a* on c_v power law dependence can be even slower.[28] The dependence on concentration of the hexagonal unit cell *a* (Figure 6) shows that the rods move apart as dilution proceeds; however, the c_v dependence is ca. $-1/8$, which suggests that the aggregates have a finite length and that they grow as a function of the concentration and/or are subjected to anisotropic swelling.

Self-Assembly in Solutions of 8-Substituted Derivatives. In the 8-unsubstituted guanosines, the base can adopt a syn or an anti orientation depending on the environment.[4,5,8] In particular, structures based on G-quartets show an alternation of both conformations, as the base is substantially free to rotate. In the ribbon structure, only the anti conformation has been observed.

8-Bromoguanosine Derivative 8. 8-bromoguanosine is reported to adopt a syn conformation in the crystalline state.[19] This conformation appears to be the most abundant one also in acqueous solution on the basis of simple NMR chemical shift considerations,[20] and has been confirmed here via HSQMBC experiments.[29] These experiments indicate a predominant syn conformation also for derivative **8** in $CDCl_3$ and DMSO-d_6 solution. NMR data in $CDCl_3$ solutions do not show broadening of the bands even at high concentrations, providing evidence that no large species are formed (in contrast, broadening of the bands was observed for G-derivatives forming ribbons and LC phases). With respect to the spectrum recorded in DMSO-d_6, $CDCl_3$ solutions exhibit a downfield shift of the H(1) proton signal (singlet), indicating the formation of hydrogen bonding,

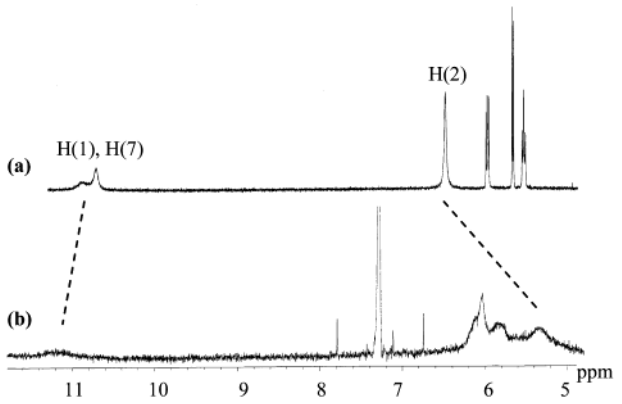

Figure 8. Room temperature H NMR spectra of derivative **6** in (a) DMSO-d_6 and (b) $CDCl_3$.

whereas the H(2) protons (also singlet) are shifted slightly upfield. NMR spectra recorded at low temperature first show broadening of the H(2) signal, which eventually splits into two signals at δ 8.50 (H-bonded) and δ 5.44 ppm (free) (see the Supporting Information). This behavior is substantially identical to that observed in ref 6 for the generation of free quartets from **4**. The NMR lines are, in all cases, sharp. This, together with the absence of LC phases, indicates that the G-quartets formed from **8**, without metal templates, do not stack to give large columnar aggregates. These data also demonstrate that the energy price required for **8** to adopt an anti conformation, necessary for ribbon formation, is not compensated by the hydrogen bonds formed in this arrangement.[6]

8-Methylthio Derivative 7. A behavior similar to **8** was observed also for 8-methylthio derivative **7** in which the splitting of the H(2) signal occurs at a temperature (-90 °C in CD_2Cl_2) lower than that of the 8-bromo derivative. Also in this case, NMR spectra in $CDCl_3$ do not show line-broadening on changing the concentration; the formation of lyomesophases has not been observed either.

Therefore, the absence of self-assembled ribbon structures and the formation of G-quartets, without metal templates, seems to be a quite general behavior for 8-substituted guanosines.[6]

8-Oxo Derivatives 5 and 6. The 8-oxo compounds show at every concentration (10^{-4}–10^{-2} mol L^{-1}) and temperature (10–45 °C) investigated very broad NMR signals in $CDCl_3$ (trace b in Figure 8). Moreover, signals in the spectra recorded in CD_2ClCD_2Cl at higher temperatures are also very broad. Thus, no detailed information on solution conformation can be obtained. However, some information can be deduced from NMR, starting from the spectrum in pure DMSO-d_6, by titration with $CDCl_3$. In pure DMSO (trace a in Figure 8), the H(1) and H(7) amide protons are nearly superimposed at δ 10.8 ppm, whereas the exocyclic H(2) amino protons are at δ 6.5 ppm. By adding $CDCl_3$, the spectrum is unchanged until a high percentage (97, 98, 99%) of $CDCl_3$ is present: at these concentrations, the H(2) amino protons undergo a large upfield shift (ca. 1.2 ppm), while the H(1) and H(7) amidic protons eventually form a broad band at ca. δ 11.2 ppm.[30] These data indicate that the NH_2 group is not involved in H-bonding, whereas the lactam groups are involved in H-bonding. Furthermore, the large upfield shift of the amino protons supports the presence of a stacked supramolecular structure.

CD spectra of derivative **6** under different experimental conditions have been recorded (Figure 9). Although the CD

(26) The best fit lines have been obtained by using a modified form of eq 1, which include the possibility of a not uniform swelling in the three dimensions, as expressed by $L/C = R\kappa/a$. The fitting equation is then $a = R\,(2\pi/\sqrt{3})^{1/3}\,\kappa^{1/3}\,c_v^{-\mu}$. The fitting parameters were $R\kappa^{1/3} = 19.9$ Å and $\mu = -0.12$ for derivative **5** and $R\kappa^{1/3} = 17.1$ Å and $\mu = -0.12$ for derivative **6**. Note that *R* is expected to be not higher than 10–12 Å: therefore, the κ values are larger than 1 and indicate that the swelling mainly occurs at the end-to-end distance between the helices.

(27) The volume of the guanosine derivatives was estimated by summing up the value of the base, the sugar moiety and the chains. As a reference, the specific volume of guanylic acid is 0.651 cm^3/g (Iball, J.; Morgan, C. H.; Wilson, H. R. *Nature* **1963**, *199*, 688).

(28) Amaral, L.; Gulik, A.; Itri, R.; Mariani, P. *Phys. Rev. A* **1992**, *46*, 3548. Mariani, P.; Amaral, L. Q. *Phys. Rev. E* **1994**, *50*, 1678.

(29) $^3J_{CH}$ coupling constants (Williamson, R. T.; Márquez, B. L.; Gerwick, W. H.; Kövér, K. E. *Magn. Res. Chem.* **2000**, *38*, 265) between H_1' and C_4/C_8 in $CDCl_3$ and DMSO-d_6 for compound **8** were 5.13/3.83 and 4.75/4.32 Hz, respectively. These values agree with a syn conformation according to the theoretical DFT Karplus relationships for unsubstituted guanosine proposed by Munzarová and Sklenář (Munzarová, M. L.; Sklenář, V. *J. Am. Chem. Soc.* **2003**, *125*, 3649).

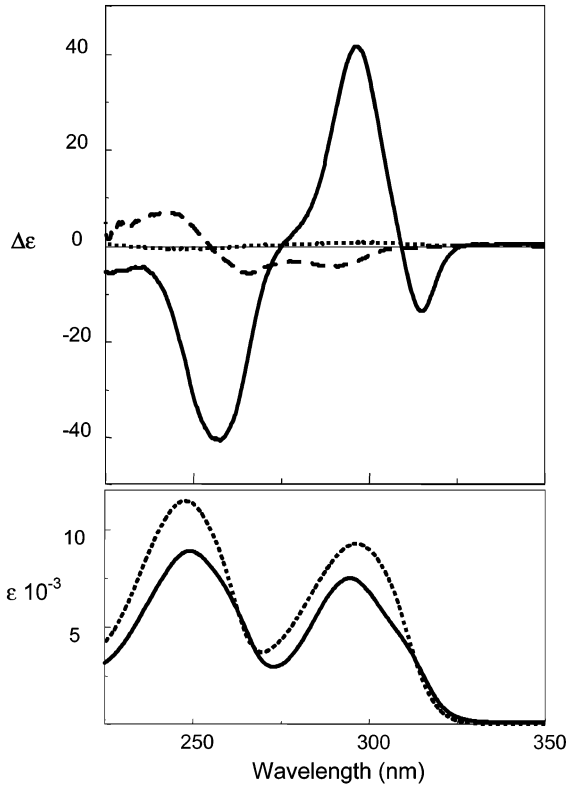

Figure 9. CD and absorption spectra of **6** in methanol (dotted line), and hexane (full line), $c = 0.5$ mM. As a comparison, the CD spectrum of the quartet-based columnar aggregate obtained in CCl_3CH_2Cl from **1** in the presence of K^+ (dashed line) is reported.[25]

signal is very weak in methanol, the bands are more intense in chloroform (not shown). In hexane, below the critical concentration for obtaining the first mesophase, the CD spectrum is dramatically different and characterized by very intense bands. The latter spectrum does not change with concentration in the range 0.05−5 mM, indicating that the population of the chirally assembled species is independent of concentration. At concentrations higher than the critical concentration, the intensity further increases and all bands are monosignated, a typical behavior for a cholesteric phase.[31]

As the assignments of the electronic transitions of 8-oxoguanine are not available, no detailed analysis of the CD spectrum can be attained. Nevertheless, a few issues can be considered:

(i) The intensity of the features in hexane (but also in chloroform) is remarkable and compatible only with a "highly" chiral structure.

(ii) The intensity does not change with concentration (below the critical concentration) or temperature, indicating a notable stability of the architecture.[32]

(iii) The g-factor (ratio between CD and absorption intensities) for the 8-oxo compound **6** is much higher than for the chiral columnar structures of guanosine derivatives based on a pile of

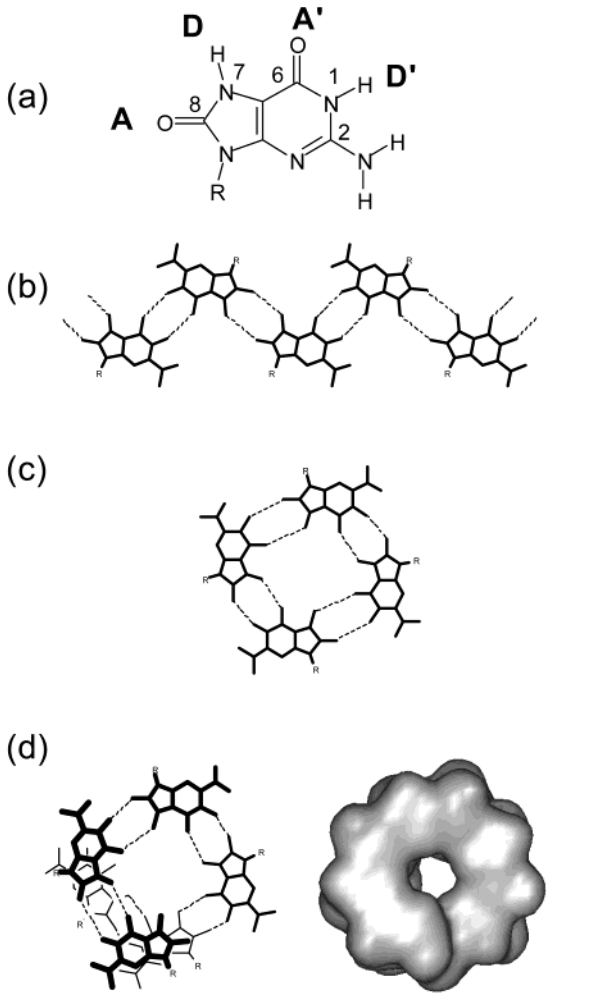

Figure 10. Donor/acceptor amide groups in the 8-oxoguanine moiety (a); architecture of the ribbonlike structure (b), the 8-oxo G-quartet (c) and the helical structure (d).

G-quartets (see Figure 9). On the other hand, guanosine ribbons display only a very weak CD spectrum.

In the case of guanine columns, a detailed analysis of the CD spectrum was reported:[33] CD bands are associated with exciton coupling of in-plane polarized transitions of adjacent quartets. Because out-of-plane polarized transitions with high intensity are unlikely also for the 8-oxo derivative, the chiral structure detected here does not seem to be composed of a stack of 8-oxo G-quartets, because a similar structure should display CD spectra with intensities similar to those of G-stacks.

The tautomeric form of the five membered ring of 8-oxo derivatives is a lactam.[34] We have, therefore, two amide-like groups present in **5** and **6** (Figure 10). This opens up new possibilities for the formation of strong amide-amide hydrogen bond pairings that are not possible in guanine.[35] In particular,

(30) The possible existence of tautomers has been taken into account, but no evidence for such equilibria has been observed. In particular, NOESY and ROESY spectra of 2-*N*-3′,5′-*O*-tripropanoyl-8-oxo-2′-deoxyguanosine showed a strong cross-peak between H(1) and H(2) and no cross-peaks relating H(7) with any sugar protons. Furthermore, no significant shift of the relevant protons was observed for **5** and **6** at different temperatures, whereas integration of each of these signals accounted satisfactorily for the expected number of protons.

(31) Gottarelli, G.; Spada, G. P. In *Circular Dichroism: Principles and Applications*; Berova, N., Nakanishi, K., Woody, R., Eds.; Wiley: New York, 2000; p 547.

(32) Even if the length of the supramolecular helix is undetermined and/or possibly changing with concentration, the intensity and shape of the CD spectrum is not expected to vary with this length. This was observed for "covalent" polymers, e. g. polypeptides (Sreerama, N.; Woody, R. W. In *Circular Dichroism: Principles and Applications*; Berova, N., Nakanishi, K., Woody, R., Eds.; Wiley: New York, 2000; p 601) and DNA (Johnson, W. C. In *Circular Dichroism: Principles and Applications*; Berova, N., Nakanishi, K., Woody, R., Eds.; Wiley: New York, 2000; p 703).

(33) Gottarelli, G.; Masiero, S.; Spada, G. P. *Enantiomer* **1998**, *3*, 429.

(34) Uesugi, S.; Ikrhara, M. *J. Am. Chem. Soc.* **1977**, *99*, 3250. Culp, S. J.; Cho, B. P.; Kadlubar, F. F.; Evans, F. E. *Chem. Res. Toxicol.* **1989**, *2*, 416.

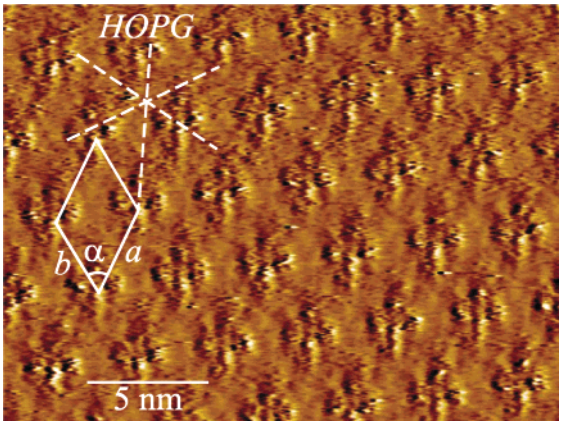

Figure 11. STM current image of **5** at the solid−liquid interface. Dashed lines indicate the HOPG axis underneath. Bias voltage 0.684 V (tip positive); average tunneling current 21 pA; scan rate 14 line/s.

amide−amide interaction can be of two types: (i) the lactam in the six-membered ring is bound to those in the six-membered ring, and those in the five-membered rings are bound similarly, leading to the generation of a ribbonlike structure (Figure 10b); and (ii) formation of H-bonds between five- and six-membered rings. This latter arrangement leads to either a quartet (Figure 10c) or to a continuous helix (Figure 10d).

Our data suggest that the helix is the most likely supramolecular structure for the 8-oxo derivatives **5** and **6**. Another piece of evidence in support of a helix comes from the fact that the quartets of 8-methylthio and 8-bromo derivatives (**7** and **8**), as well as that reported by Sessler (**4**),[6] without added ions do not stack to form a columnar structure. Therefore, a pile of quartets (Figure 10c) without metal templates seems very unlikely for **5** and **6**.[36]

Self-Assembly at Surfaces. Figure 11 displays the constant height STM image of **5** at the graphite-solution interface. It reveals an array of quartets that are packed according to a unit cell of $a = (3.8 \pm 0.2)$ nm, $b = (3.4 \pm 0.2)$ nm, $\alpha = (59 \pm 3)°$. This is consistent with a hexagonal motif. The *a* vector is at 22° from the nearest neighbor axis in the HOPG lattice (see dashed lines).[37] The bright spots corresponding to higher tunneling probability can be assigned to the conjugated guanine core since the energy difference between their HOMO and the Fermi-level of HOPG is smaller than for the sugar and for the aliphatic side chains.[38]

The visualized quartet is not in disagreement with the helical models as it could represent a section of a helical architecture (ca. four repeats per turn, Figure 10d). Note that by selecting the tunneling parameters in STM experiments at the solid−liquid interface, one can tune the tip−substrate gap, allowing one or more adlayers to fit in the gap and scraping away the upper layers. In this way, one would shave off part of the helix, obtaining a section that can appear in STM imaging as a quartet array of bright spots.

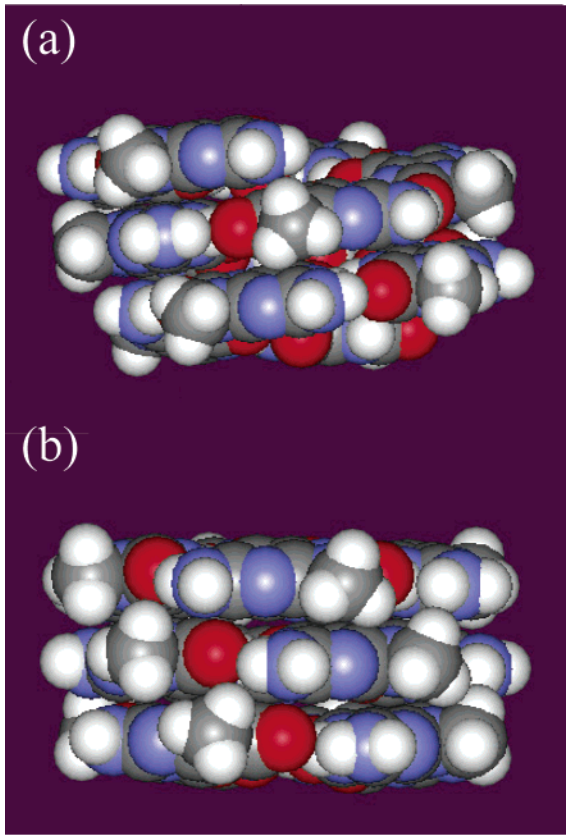

Figure 12. CPK models of a continuous helix (a) and of a stacked quartet-based assembly (b) formed by twelve molecules of the model 9-methyl-8-oxoguanine.

Discussion

The 8-oxoguanosine derivatives **5** and **6** could self-assemble under diverse environments according to different motifs (shown in Figure 10). A careful examination of the data reported above indicates that the continuous helix must be the most populated structure because of the following:

(i) The structure of the cholesteric and hexagonal liquid crystalline phases is typical of columnar aggregates, and not of flat ribbonlike structures. On the other hand, other authors,[10] as well as our group have never found cholesterics or hexagonal LCs with ribbon like architecture.

(ii) As indicated by Sessler's results,[6] and those presented in this work, classical G-quartets are unable to give columnar aggregates by stacking in the absence of metal templates.

(iii) The CD spectrum strongly indicates a helical structure.

(iv) Only a subtle structural deformation is needed to change a planar quartet into a continuous helix. The formation of a continuous helix, rather than a stack of G-quartets in the case of guanosine-5′-phosphate has been proposed.[39] The structures obtained after molecular dynamics calculations of two assemblies of twelve molecules of 9-methyl-8-oxoguanine are displayed in Figure 12: the energy of the two structures is the

(35) Pranata, J.; Wierschе, S. G.; Jorgensen, W. L. *J. Am. Chem. Soc.* **1991**, *113*, 2810.
(36) Extraction experiments of aqueous potassium (or sodium) picrate with **5** gave negative results. It is therefore very unlikely that 8-oxo compounds can capture Na^+ or K^+ from the surroundings. Furthermore, in ESI−MS we have not observed signals corresponding to $[M + Na]^+$ species. $[M + Na]^+$ species were instead observed for compound **1**.
(37) The STM visualization of the missing quartet in the self-assembled crystal (see the Supporting Information) provides unambiguous evidence that the visualized arrangement is not an imaging artifact.
(38) Lazzaroni, R.; Calderone, A.; Brédas, J. L.; Rabe, J. P. *J. Chem. Phys.* **1997**, *107*, 99.
(39) Walmsley, J. A.; Burnett, J. F. *Biochemistry* **1999**, *38*, 14 063. Davies, D. R. *Annu. Rev. Bioch.* **1967**, *36*, 321. Sasisekharan, V.; Zimmerman, S. B.; Davies, D. R. *J. Mol. Biol.* **1975**, *92*, 171. Audet, P.; Simard, C.; Savoie, R. *Biopolymers* **1991**, *31*, 243.

same (within the method accuracy).[40] There are, therefore, no compelling energetic reasons for choosing the quartet structure.

Moreover, we have previously shown that placing the 8-oxo assembled species between two facing Au electrodes, gives a hybrid system that displays rectifying electrical behavior.[13,41] This rectification requires a dipolar character for the supramolecular architecture, which would exist in a helix but would be very unlikely in a stack of quartets.

Conclusions

In summary, the cooperative effect of hydrogen bonding and solvophobic interactions induces the 8-oxoguanosines **5** and **6** to self-associate into a helical architectures both in the liquid crystalline phase, in solution and at surfaces. These arrangements, which are markedly different from the structures obtained by the spontaneous self-assembly of guanosine derivatives unsubstituted at the C(8) position, are of interest, not only for their optical properties, but also for their ability to rectify currents, making them potential building blocks for the construction of nanoscale bio-electronic devices and circuits.

Experimental Procedures

CD spectra were recorded with a JASCO J-710 spectropolarimeter using cells of the appropriate path-length. NMR spectra were recorded with Varian instruments at 300 or 400 MHz.

X-ray diffraction experiments were performed using a 3.5 kW Philips PW1830 X-ray generator equipped with a Guinier-type focusing camera operating in a vacuum: a bent quartz crystal monochromator was used to select the Cu−$K_{\alpha 1}$ radiation ($\lambda = 1.54$ Å). The explored s range extended from 0.01 to 0.35 Å^{-1} ($s = 2 \sin \theta/\lambda$, where 2θ is the scattering angle). The samples were mounted in a vacuum-tight cells with thin mica windows. To reduce the spottiness arising from possible macroscopic monodomains, the cells were continuously rotated during exposure. The sample cell temperature was controlled with an accuracy of 0.5 °C by using a circulating thermostat. The diffraction patterns were recorded on a curved detector INEL CPS120. In each experiment, a number of sharp or broad reflections were observed and their spacings measured following the usual procedure. In some cases, the X-ray diffraction profiles were recorded after solvent loss due to partial evaporation in order to follow the general trend of the structural parameters. Therefore, in such cases, the sample concentration, which was determined by gravimetric measurements, is only indicative.

The STM investigation has been carried out at the solid−liquid interface[42] using a picoAmp Nanoscope IIIa setup (Digital Instrument) with the E scanner. Pt/Ir (85−15%) tips have been prepared from a 0.25 mm thick wire by mechanical cutting or by electrochemical etching using a solution of NaCN (6 N) + KOH (2 N). Almost saturated solutions of **5** in 1,2,4-trichlorobenzene have been applied to the basal plane of the freshly cleaved highly oriented pyrolitic graphite (HOPG) substrate. The lattice of the underlying HOPG has been monitored during the measurements by simply changing the tunneling parameters; this permitted the calibration of the piezo in the *xy* plane in situ. Unit cells were averaged on several images after their correction for the piezo drift (using SPIP Scanning Probe Image Processor, Version 1.720, Image Metrology ApS, Lyngby, Denmark). STM current images with a submolecular resolution have been recorded using average tunneling currents (I_t) = 10−30 pA, tip voltage (U_t) = 0.4−1.2 V and scan rates = 10−30 lines/s.

3′,5′-*O*-Didecanoyl-8-oxo-2′-deoxyguanosine (5). 8-Oxo-2′-deoxyguanosine (Berry & Associate) (0.53 mmol) was dried over P_2O_5 in vacuo for 2 h at 50 °C and then suspended in MeCN (12 mL). Redistilled Et_3N (1.2 mmol), DMAP (0.1 mmol) and decanoic anhydride (1.17 mmol) were added, and the resulting mixture was stirred overnight at r.t. Methanol (0.5 mL) was then added, and stirring was continued for 20 min. The mixture was filtered and the precipitate washed several times with small portions of MeCN and Millipore H_2O to afford analytically pure **5** as a white solid in a 25% yield. ^{1}H NMR (200 MHz, DMSO-d_6): 0.98 (t, 6H Me); 1.25 (m, 12H aliphatic CH_2's); 1.55 (m, CH_2CO); 2.30 (dd, H2′); 3.28 (m, H2′); 4,05−4.19 (m, H4′, H5′); 4.35 (m, H5′); 5,39 (m, H3′); 6.02 (t, H1′); 6.49 (bs, NH_2); 10.75 (s, NH). ESI-MS ($CHCl_3$/MeOH): 590.10 (100, [**5**−H]$^-$).

2′,3′,5′-*O*-Tridecanoyl-8-oxoguanosine (6). 8-Oxoguanosine was obtained by catalytic hydrogenation[43] (10% Pd/C) of benzyloxy derivative[44] in EtOH−H_2O (1:1, v/v). 8-Oxoguanosine (218 mg, 0.73 mmol) was dissolved in 12 mL of anhydrous acetonitrile. To this solution distilled triethylamine (2.1 mmol), decanoic anhydride (2.1 mmol) and a catalytic amount of DMAP were added. The mixture was stirred for 12 h at r.t. and the crude, after evaporation in vacuo of the solvent, was applied to a silica gel column. After washing with a mixture of dichloromethane-acetone (9:1), to remove the decanoic acid, 2′,3′,5′-*O*-tridecanoil-8-oxoguanosine was eluted with a mixture of dichloromethane−methanol (95:5). The product, after evaporation of the solvent, was crystallized from methanol to give 0.12 g (0.16 mmol, 22% yield). ^{1}H NMR (200 MHz, DMSO-d_6): 10.84 (s, 2H, NH), 6.53 (bs, 2H, NH_2), 6.02 (m, 1H, H2′), 5.70 (d, 1H, H1′), 5.57 (t, 1H, H3′), 4.35 (m, 1H, H5′), 4.21−4.08 (m, 2H, H4′-H5′′), 2.39−2.23 (m, 6H, CH_2CO), 1.60−1.38 (m, 6H, CH_2−CH_2CO), 1.34−1.12 (m, 36H, CH_2), 0.85 (t, 9H, CH_3). ESI-MS ($CHCl_3$/MeOH): 761.1 (100, [**6**−H]$^-$).

2′,3′,5′-*O*-Tridecanoyl-8-methyltioguanosine (7). 8-Mercaptoguanosine (Sigma) (0.95 mmol) was dried over P_2O_5 in vacuo for 2 h at 50 °C and then suspended in DMF (4.5 mL) in the presence of K_2CO_3 (1.24 mmol). Dimethyl sulfate (1.14 mmol) was added and the resulting mixture was stirred for 3 h at 75 °C. The reaction mixture was then cooled, and acetone (60 mL) was added. The reaction mixture was filtered and the precipitate was re-crystallized from water to afford analytically pure 8-methyltioguanosine as a white solid in a 63% yield. ESI−MS (MeOH): 328.0 (100, [M−H$^+$]). The product was used in the subsequent step without any further purification. 8-Methyltioguanosine (0.85 mmol) was dried over P_2O_5 in vacuo for 2 h at r.t. and then suspended in MeCN (15 mL). Redistilled Et_3N (2.79 mmol), DMAP (0.1 mmol) and decanoic anhydride (2.79 mmol) were added, and the resulting mixture was stirred for 5 h at RT. Methanol (1 mL) was then added, and stirring was continued for 20 min. The mixture was concentrated and then chromatographed on silica (eluent: dichloromethane/methanol from 99:1 to 97:3) to afford analytically pure **7** in a 50% yield. ^{1}H NMR (200 MHz, $CDCl_3$): 0.98 (m, 9H, Me); 1.33−2.41 (m, 24H, CH_2); 2.75 (s, 3H, MeS); 4,31−4.37 (m, H4′, H5′); 4.51 (m, H5′); 5,73 (bs, NH_2); 5.91−5.94 (m, H3′, H1′); 6.14 (dd, H2′); 12.2 (s, NH). ESI−MS ($CHCl_3$/MeOH): 790.8 (100, [**7**−H]$^-$).

2′,3′,5′-*O*-Tridecanoyl-8-bromoguanosine (8). 8-Bromoguanosine[45] (600 mg, 1.66 mmol) was dissolved in 10 mL of anhydrous acetonitrile.

(40) Calculations were performed with MacroModel 7.0 (Schrödinger) using a stochastic dynamics method with the force field AMBER* in vacuo at constant temperature (300 K).

(41) In the experiments reported in ref 13, the gold nanoelectrodes are at a distance of 60 nm and probe an array of helical structures, which are very probably, though not necessarily, disordered. In the case of G-ribbons,[12−14] in the crystal structure the ribbons are dipolar and the dipoles are parallel to each other. Unfortunately, we do not have the crystal structure of the present 8-oxoguanosine derivatives, but the helices do not necessarily have to be antiparallel.

(42) Rabe, J. P.; Buchholz, S. *Science* **1991**, *253*, 424. Cyr, D. M.; Venkataraman, B.; Flynn, G. W. *Chem. Mater.* **1996**, *8*, 1600. Claypool, C. L.; Faglioni, F.; Goddard, W. A., III; Gray, H. B.; Lewis, N.; Marcus, R. A. *J. Phys. Chem. B* **1997**, *101*, 5978. Qiu, X.; Wang, C.; Zeng, Q.; Xu, B.; Yin, S.; Wang, H.; Xu, S.; Bai, C. *J. Am. Chem. Soc.* **2000**, *122*, 5550. Gesquière, A.; Abdel-Mottaleb, M. M. S.; De Feyter, S.; De Schryver, F. C.; Schoonbeek, F.; van Esch, J.; Kellogg, R. M.; Feringa, B. L.; Calderone, A.; Lazzaroni, R.; Brédas, J. L. *Langmuir* **2000**, *16*, 10385. Isoda, S.; Nemoto, T.; Fujiwara, E.; Adachi, Y.; Kobayashi, T. *J. Crys. Growth* **2001**, *229*, 574. Samorí, P.; Rabe, J. P. *J. Phys.: Cond. Matter* **2002**, *14*, 9955.

(43) Bowles, W. A.; Schneider, F. H.; Lewis, L. R.; Robins, R. K. *J. Med. Chem.* **1963**, *6*, 471.

(44) Ikehara, M.; Muneyama, K. *Chem. Pharm. Bull.* **1966**, *14*, 46. Holmes, R.; Robins, R. K. *J. Am. Chem. Soc.* **1965**, *87*, 1772.

To this solution was added distilled triethylamine (4.98 mmol), decanoic anhydride (4.98 mmol), and a catalytic amount of DMAP. The mixture was stirred for 12 h. at RT, and the crude, after evaporation in vacuo of the solvent, was applied to a silica gel column. After washing with a mixture of dichloromethane-acetone (9:1), to remove the decanoic acid, 2′,3′,5′-*O*-tridecanoyl-8-bromoguanosine was eluted with a mixture of dichloromethane-methanol (95:5). The product, after evaporation of the solvent, was crystallized from ethanol to give 0.6 g (0.70 mmol, 42% yield) of the title compound as a white solid. ^{1}H NMR (200 MHz, DMSO-d_6): 11.00 (s, 1H, NH), 6.61 (bs, 2H, NH_2), 6.02 (m, 1H, H2′), 5.84 (d, 1H, H1′), 5.67 (t, 1H, H3′), 4.45−4.17 (m, 3H, H5′, H5″, H4′), 2.40−2.22 (m, 6H, CH_2CO), 1.53−1.46 (m, 6H, CH_2−CH_2CO), 1.24−1.20 (m, 36H, CH_2), 0.84 (t, 9H, CH_3). ESI−MS ($CHCl_3$/MeOH): 823.1, 825.1 (47, 53 [**8**−H]$^-$).

(45) Long, R. A.; Robins, R. K.; Townsend, L. B. In *Synthetic Procedures in Nucleic Acid Chemistry*; Zorbach, W. W., Tipson, R. S., Eds.; Wiley-Interscience: New York, 1968; Vol. 1, p 228.

Acknowledgment. This paper is dedicated to Professor Stephen F. Mason on the occasion of his 80th birthday. This work has been supported by MIUR (PRIN 2001 project), FIRB (Nomade project) and the University of Bologna. Research in Berlin on the self-assembly of supramolecular nanostructures was financed by the EU-TMR project SISITOMAS (project reference FMRX970099). Moreover, support from the British−Italian Partnership Program (British Council−CRUI) is gratefully acknowledged. We thank Dr. Paola Franchi (University of Bologna) for molecular dynamics calculations.

Supporting Information Available: H NMR spectra of **8** and a STM current image of **5**. This material is available free of charge via the Internet at http://pubs.acs.org.

JA0364827